Frontiers in Bioscience Landmark

Front. Biosci. (Landmark Ed). **2022**; 27(1): 025
http://doi.org/10.31083/j.fbl2701025

Original Research

Effect of gigantol on the proliferation of hepatocellular carcinoma cells tested by a network-based pharmacological approach and experiments

Shujie Li[1,2,†], Hualing Li[3,†], Dandan Yin[4,†], Xiaojing Xue[5], Xiaoling Chen[2], Xiaoyue Li[1], Junwei Li[6,*], Yongxiang Yi[1,*]

[1]Department of Hepatobiliary Surgery, The Second Hospital of Nanjing, Nanjing University of Chinese Medicine, 210003 Nanjing, Jiangsu, China
[2]Department of Traditional Chinese Medicine, Fujian Medical University Union Hospital, 350000 Fuzhou, Fujian, China
[3]Fuqing Li Hualing TCM Clinic, 350000 Fuzhou, Fujian, China
[4]Clinical Research Center, The Second Hospital of Nanjing, Nanjing University of Chinese Medicine, 210003 Nanjing, Jiangsu, China
[5]Department of neurology, Fujian Provincial Hospital, 350000 Fuzhou, Fujian, China
[6]Department of Infectious Diseases, The Second Hospital of Nanjing, Nanjing University of Chinese Medicine, 210003 Nanjing, Jiangsu, China
*Correspondence: njyy042@njucm.edu.cn (Yongxiang Yi); Junwli@yeah.net (Junwei Li)
[†]These authors contributed equally.
Academic Editor: Josef Jampilek
Submitted: 25 October 2021 Revised: 6 December 2021 Accepted: 22 December 2021 Published: 17 January 2022

Abstract

Background: Hepatocellular carcinoma (HCC) is a common clinical malignant disease and the second leading cause of cancer-related death worldwide. Dendrobium is a commonly applied nourishing drug in traditional Chinese medicine. Gigantol is a phenolic compound extracted from Dendrobium. The compound has attracted attention for its anticancer effects. However, the mechanism of gigantol in HCC has not been extensively explored. **Methods**: Potential targets of gigantol were predicted by SwissTargetPrediction. HCC-related genes were obtained from the GeneCards, Online Mendelian Inheritance in Man (OMIM), Pharmacogenetics and Pharmacogenomics Knowledge Base (PharmGKB), Therapeutic Target Database (TTD) and DrugBank databases. The "gigantol-target-disease" network was constructed using Cytoscape software. Protein interaction network analysis was performed using STRING software. Gene Ontology (GO) and Kyoto Encyclopedia of Genes and Genomes (KEGG) pathway analyses were executed utilizing the *R* package to explore the possible regulatory mechanisms of gigantol in HCC. To authenticate the role of gigantol in HCC, Cell Counting Kit-8 (CCK-8) assay, 5-ethynyl-2'-deoxyuridine (EdU) assay, wound healing assay, Matrigel invasion assay and Western blot were performed. **Results**: Three core genes were screened from 32 closely linked genes. Pathway analysis yielded many signaling pathways associated with cancer. The CCK-8 assay and EdU assay indicated that gigantol suppressed the growth of HCC cells. The wound healing assay and Matrigel invasion assay showed the inhibition of migration and metastasis of HCC cells by gigantol. We verified from molecular docking and protein level that gigantol can exert regulatory effects through three targets, ESR1, XIAP and HSP90AA1. Furthermore, Western blot results tentatively revealed that gigantol may inhibit HCC progression through the HSP90/Akt/CDK1 pathway. **Conclusions**: Our results confirms anti-HCC proliferation activity of gigantol through PI3K pathway described in existing literature by different experimental approaches. Furthermore, it has discovered other proteins regulated by the drug that was not previously reported in the literature.These findings provide potential molecular and cellular evidence that gigantol may be a promising antitumor agent.

Keywords: Gigantol; Hepatocellular carcinoma; Network-based pharmacological; Molecular docking; Anti-HCC effect

1. Introduction

Hepatocellular carcinoma is currently the fifth most common malignancy worldwide and the second leading cause of death from cancer [1]. The pathological types of primary liver cancer mainly include hepatocellular carcinoma, intrahepatic cholangiocarcinoma, and mixed hepatocellular carcinoma, of which HCC accounts for approximately 85%–90%. HCC mostly emerges from chronic liver disease or cirrhosis and has an insidious onset. Early symptoms are not always obvious, so most patients are diagnosed at a late stage, resulting in a very poor overall prognosis. The treatment of HCC emphasizes an integrated, multidisciplinary model to improve patient survival. For inoperable HCC, radiation therapy (radiotherapy) [2,3], radiofrequency ablation (RFA) [4–8], transarterial chemoembolization (TACE) [9–11], and systemic therapy are all effective treatment options [12–16]. Therefore, the study of valuable therapeutic agents will help improve the clinical outcome of patients.

Dendrobium is listed in Shen Nong Ben Cao Jing (The Divine Husbandman's Classic of Materia Medica) and is classified as a top quality plant as a perennial green herb of the orchid family. The Chinese Pharmacopoeia records that Dendrobium is cold in nature, sweet, light and salty in taste, and enters the stomach, lung and kidney meridians. Due to benefiting the stomach and generating fluid, nourishing Yin and clearing heat. Research has confirmed that many compounds in Dendrobium, especially the bibenzyl and phenolic compounds, have significant antitumor activ-

ity and antimultidrug resistance and have inhibitory effects on many human tumor cell lines [17]. Gigantol is a typical phenolic compound in Dendrobium, and some studies have shown that gigantol can inhibit the oxidative stress induced by high sugar and may have a protective effect in the development of diabetic retinopathy, which may help reduce neovascularization [18]. Gigantol inhibits stem cell protein kinase B (Akt) signaling in cancer cells by reducing lung cancer activity, thereby reducing the cellular levels of pluripotency and the self-renewal factors Oct4 and Nanog [19]. Gigantol dramatically reduces the viability of lung cancer cells in the isolated state [20]. Therefore, gigantol may be developed as a therapeutic agent for cancer.

Network pharmacology is an effective method to study the multicomponent and multitarget mechanism of Chinese herbal compounds and is holistic, systematic and connected and coincides with the theory of a holistic view, diagnosis and treatment, and prescription dispensing in Chinese medicine [21–24]. In this study, we aimed to construct a "compound-target-disease" network based on network pharmacology and explore the molecular mechanisms and pathways of gigantol in the treatment of HCC through molecular docking and *in vitro* validation.

2. Materials and methods

2.1 Construction of "drug-target-disease" network

Structural information on gigantol (CAS:67884-30-4) was obtained from NCBI PubChem (https://pubchem.ncbi.nlm.nih.gov/) [25]. Swiss absorption, distribution, metabolism and excretion (SwissADME), was used to identify the bioavailability and metabolism of gigantol [26]. Additionally, the protein targets of this compound were retrieved from SwissTargetPrediction with a probability value $\geq$0.5. Data on hepatocellular carcinoma-related targets were integrated from five databases using *R* Software (Lucent Technologies, Murray Hill, NJ, USA): GeneCards (https://www.genecards.org) [27], OMIM (http://omim.org) [28], PharmGKB (https://www.pharmgkb.org) [29], TTD (http://db.idrblab.net/ttd) [30], and DrugBank (https://go.drugbank.com) [31]. Common targets for gigantol and HCC were obtained using *R* packages ("Venn") (https://cran.r-project.org/web/packages/VennDiagram/index.html).

2.2 Protein interaction network construction

The common targets were uploaded to the STRING database (https://string-db.org/), and the protein interaction network was constructed with the following conditions: the species was "Homo sapiens", the minimum interaction score (medium confidence) was 0.4, and the free protein sites were removed [32]. The obtained protein interaction networks were imported into Cytoscape 3.8.2 software (Institute of Systems Biology, Boston, MA, USA) for visualization and processing analysis using the Network Analyzer module [33]. Finally, the core genes were screened by the *cytoNCA* plug-in. The *cytoNCA* plug-in performs topology analysis with a 2-fold average degree value as a filtering condition.

2.3 Gene function and pathway enrichment analysis

GO and KEGG pathway enrichment analysis were performed using the *R* package ("*clusterProfiler*" "*org.Hs.eg.db*" "*enrichplot*" "*ggplot2*" "*pathview*"). The significance values for GO terms and KEGG pathways were set at *FDR* $<$0.05 and $p < 0.05$, respectively.

2.4 Analytical molecular docking

The two-dimensional structure of gigantol were available from the PubChem website in structured data format (SDF) format [25]. The 3D structure of the core target protein was downloaded from the PDB database (https://www1.rcsb.org/) and saved in PDB format [34]. Water molecules and small molecule ligands were removed using PyMOL software (Schrödinger, New York, USA) and hydrogenated using AutoDockTools software (Scripps Research, La Jolla, CA, USA) (The PyMOL Molecular Graphics System, Version 2.0 Schrödinger, LLC) [35]. Molecular docking of the receptor and ligand was performed using Vina 1.1.2 (Scripps Research, La Jolla, CA, USA) [36]. The binding activity was evaluated by docking score values.

2.5 Cell culture

The human hepatocellular carcinoma cell lines Hep3B, SMMC-7721, and HCC-LM3 were obtained from the Chinese Academy of Sciences (Shanghai, China). Cells were cultured in Dulbecco's Modified Eagle Medium (DMEM, Gibco, Grand Island, NY, USA) supplemented with 10% FBS (Gibco, Grand Island, NY, USA) and 100 U/mL Penicillin/Streptomycin (Gibco, Grand Island, NY, USA) in a 5% CO_2 incubator. Cells undergoing a logarithmic growth period were used for follow-up experiments.

2.6 Cell viability assay

A CCK-8 assay kit was used to evaluate cell viability following the manufacturer's instructions (HY-K0301, MedChemExpress, Monmouth Junction, NJ, USA). Cells in the logarithmic growth phase were inoculated into 96-well plates (7×10^3 cells/well). After 12 h, different concentrations of gigantol (HY-N2523, MedChemExpress, Monmouth Junction, NJ, USA) were added, and 6 replicate wells were added for each group. Cells were incubated at 37 °C for 24, 48 and 72 h. The supernatant was then discarded, and the cells were washed twice with PBS. A solution of 10% CCK-8 was then added and incubated at 37 °C for 2 h. The absorption was measured at 450 nm by an microplate reader (Multiskan™ FC Microplate Photometer, ThermoFisher, Waltham, MA, USA).

2.7 EdU staining assay

A EdU detection kit (Us Everbright, Suzhou, Jiangsu, China) was used, as stated by the manufacturer's instructions, to identify the proliferating cells. SMMC-7721 and Hep3B were intervened with different concentrations of gigantol for 24 h after apposition. Appropriate amounts of cells were inoculated in 96-well plates and cultured in the logarithmic growth phase. EdU solution was diluted with complete medium at a 1000:1 ratio, 100 μL EdU medium per well, and incubated in an incubator for 2 h. After washing twice with PBS, 50 μL of 4% paraformaldehyde was added to each well and incubated at room temperature for 30 min. After washing with PBS for 5 min, 100 μL of 0.5% Triton X-100 permeate was added to each well. Next, 100 μL of Apollo staining reaction solution was added to each well. The staining solution was then incubated for 30 min at room temperature and discarded. Finally, Hoechst 33324 staining solution was added to each well and incubated for 15 min, followed by 3 washes with PBS for 5 min each. Fluorescence microscopy was performed to observe the EdU-positive cells, which were counted and statistically analyzed.

2.8 Wound healing assay

Hep3B and SMMC-7721 cells were seeded onto cell inserts (Culture-Insert 4 well, ibidi, Gräfelfing, Germany) in a 12-well plate at a density of 5×10^5 cells/mL. The insert was removed after 12 h. Subsequently, the cells were imaged under a microscope in which the 0 h results were used as control conditions. Next, the cells were processed with different concentrations of gigantol (0, 25, 50, 100 μM) for 24 h. The area ratios were imaged by microscopy after 24 hand calculated using Image J software (National Institutes of Health, Bethesda, MD, USA).

2.9 Transwell invasion assay

For the transwell invasion assay, matrigel chambers (BD Biosciences, San Jose, CA, USA) were carried out according to manufacturer's instructions. Matrigel was melted at 4 °C followed by dilution with DMEM exclusive of FBS at a concentration of 1 mg/mL. Then, 100 μL of Matrigel (1 mg/mL) was placed into the upper chamber, where it was incubated for 4 h at 37 °C until it aggregated. Hep3B and SMMC-7721 cells were cultured in serum free medium for 12 h. Cells in 200 μL of serum free medium that contained different concentrations of gigantol (0, 25, 50, 100 μM) were placed in the upper chamber. The lower chamber was filled with 600 μL of medium containing 15% FBS. Following 24 h of incubation, cells were fixed with 4% paraformaldehyde and subsequently stained with 0.1% crystal violet. Furthermore, the upper chamber was carefully cleaned with a cotton swab. The number of cells migrating to the lower surface was counted in five randomly selected fields of view ($\times$200). The results were quantified using Image J software (National Institutes of Health, Bethesda, MD, USA).

2.10 Western blot analysis

Cells in logarithmic growth phase were seeded in 6-well plates at No. 1×10^6 cells/cm^{2}and then treated with gigantol (25, 50, 100 μM) and blank control (DMSO) for 48h at 37 °C with 5% CO_2 in an incubator. Subsequently, the cells were collected and lysed using radio immunoprecipitation assay (RIPA) on ice for 30 min and centrifuged at 4 °C for 20 min at 12,000 $\times$ g. The supernatant was transferred to an EP tube. The protein concentration was measured with a BCA protein concentration assay kit (KGP902, KeyGEN BioTECH, Nanjing, Jiangsu, China). Cell lysates were then loaded into 10% SDS-PAGE gels. Proteins were transferred to polyvinylidene difluoride (PVDF) (IPVH00010, Millipore, Burlington, MA, USA) membranes and blocked with 5% skim milk in Tris-buffered saline containing 1% Tween 20 for 1 h. The PVDF membranes were then incubated with *primary antibody* at 4 °C overnight. N-cadherin *primary antibody* (1:1000, #13116, rabbit), XIAP *primary antibody* (1:1000, #2045, rabbit), HSP90 *primary antibody* (1:1000, #4877, rabbit), ESR1 *primary antibody* (1:1000, #8644, rabbit), PCNA *primary antibody* (1:1000, #13110, rabbit), phospho-Akt *primary antibody* (1:2000, #4060, rabbit), Akt *primary antibody* (1:1000, #4685, rabbit), β-actin *primary antibody* (1:1000, #4970, rabbit), E-cadherin *primary antibody* (1:1000, #3195, rabbit) and Vimentin *primary antibody* (1:1000, #5741, rabbit) were purchased from Cell Signaling technology, Inc., Danvers, MA, USA. CDK1 *primary antibody* (1:10000, ab133327, rabbit) and MCM2 *primary antibody* (1:1000, ab108935, rabbit) was purchased from Abcam (San Francisco, CA, USA). The membranes were thoroughly washed and incubated with horseradish peroxidase-conjugated secondary antibodies (1:2000, KGAA35, goat anti-rabbit IgG, KeyGEN BioTECH, Nanjing, China). Once washed, the protein bands were visualized by enhanced chemiluminescence (ECL), and the gray values of the proteins were analyzed using Image J software (National Institutes of Health, Bethesda, MD, USA).

2.11 Statistical analysis

GraphPad Prism 8.0 software (GraphPad Software, San Diego, CA, USA) for Windows was used for statistical analysis. Statistically significant differences were calculated using ANOVA. A p-value < 0.05 was accepted as statistically significant.

3. Results

3.1 Target identification

The SwissADME results indicated that gigantol not only undergoes passive gastrointestinal absorption but also crosses the BBB (Table 1) (http://www.swissadme.ch/index.php). A total of 102 gigantol-associated targets were retrieved (**Supplementary Table 1**). Subsequently, a total of 1184 hepatocellular carcinoma related target genes were

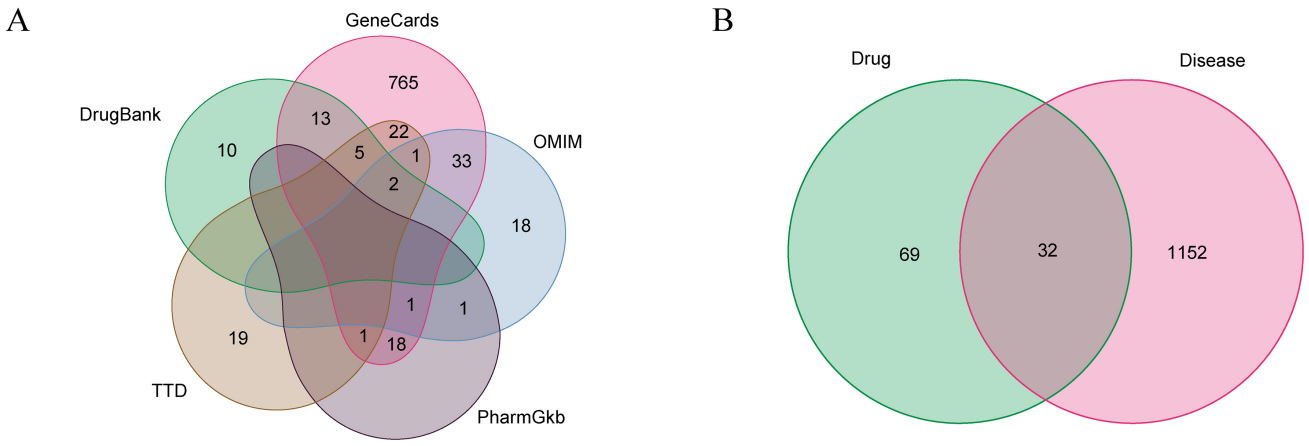

Fig. 1. Analysis of the predicted genes. (A) Intersection of HCC target genes predicted by five types of databases. (B) Venn diagram of HCC-related genes and gigantol target genes. Using *R* packages ("*Venn*").

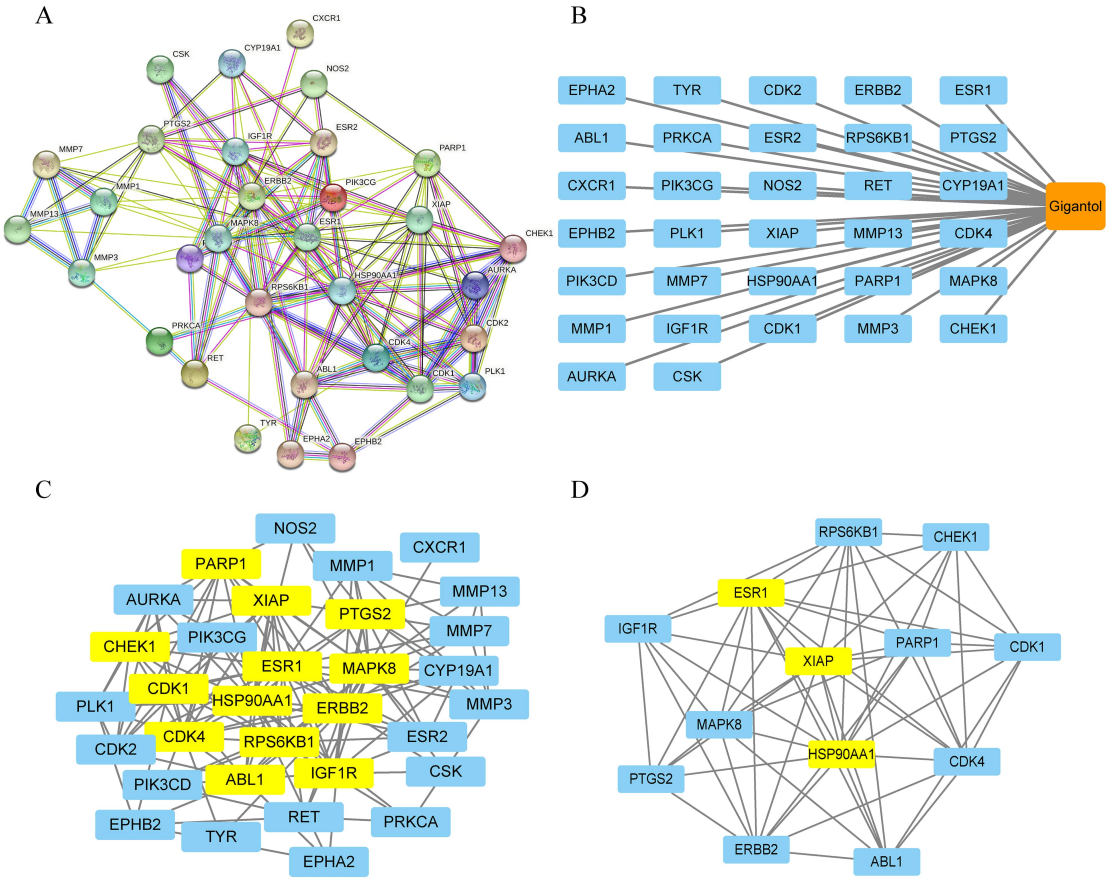

Fig. 2. Network pharmacology of gigantoland HCC. (A) The PPI network of common genes. (B) The "HCC-targets-gigantol" network. (C) Visualization of the first 13 core genes was obtained using *R* software. (D) The top 3 potential effective targets in core genes. Obtained by Cytoscape and cytoNCA plug-in analysis for mapping.

compiled from the OMIM, PharmGKB, GeneCards, TTD and DrugBank databases (Fig. 1A). Thus, we integrated the drug targets and disease targets using the *R* package "*Venn*". After eliminating duplicates, we identified 32 common targets, which are shown in Fig. 1B.

3.2 Analysis of target protein interaction network

The 32 intersecting targets were imported into the STRING database to obtain the protein interaction network and the corresponding network (Fig. 2A–B). The data were loaded into Cytoscape for visual topological analysis, and 32 nodes with 148 edges and an average de-

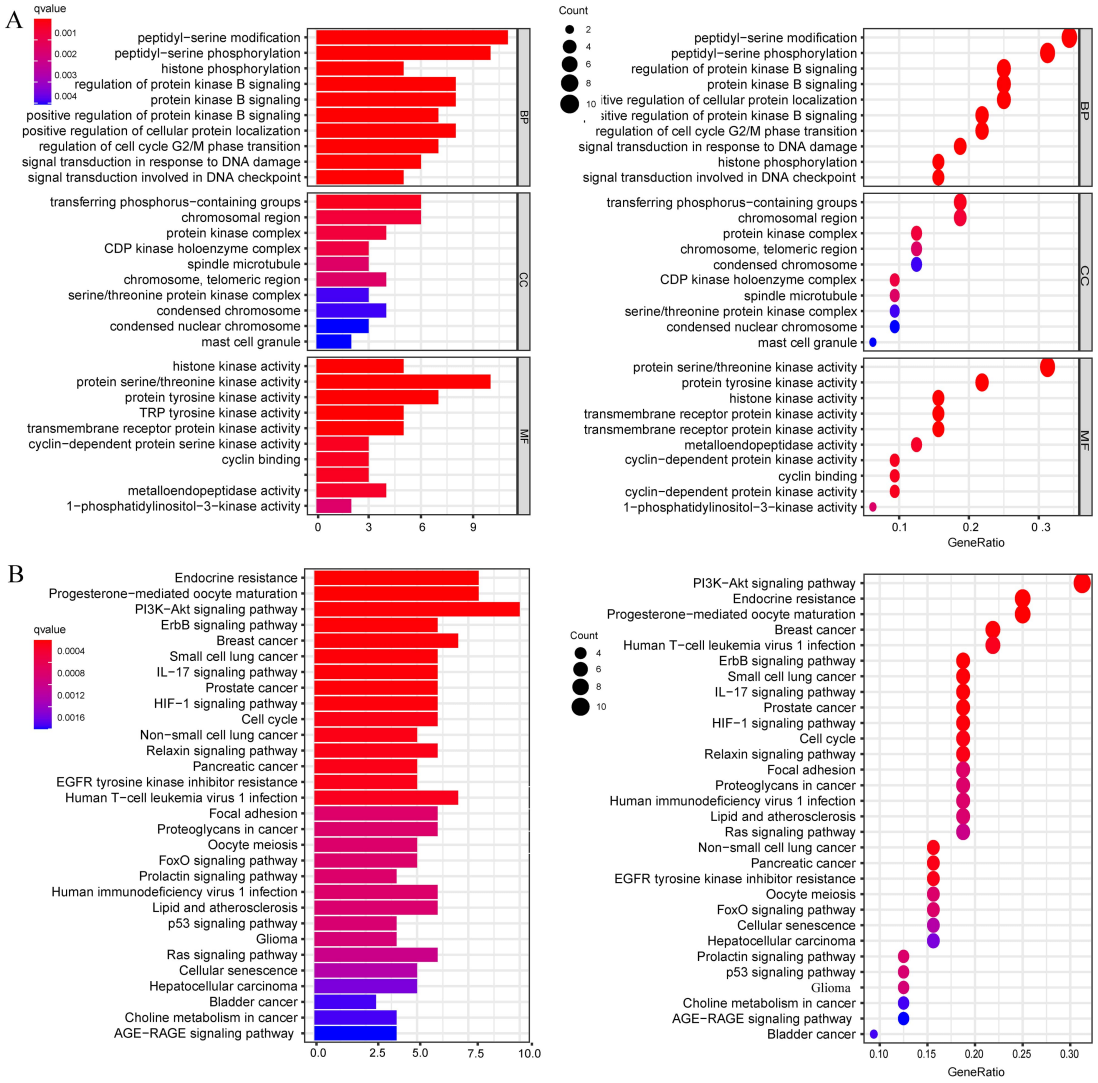

Fig. 3. Enrichment analysis of the 32 genes by GO and KEGG. (A) GO functional annotation of 32 genes of gigantol. BP, CC and MF were analyzed using *R* software. (B) KEGG pathway analysis of 32 genes and column plot for top 30 pathways. GO and KEGG analysis were performed using the *R* package (GO, KEGG: "*clusterProfiler*", "*org.Hs.eg.db*", "*enrichplot*", "*ggplot2*").

Table 1. Molecular properties of gigantol.

Property	Parameter
MW	274.31 g/mol
TPSA	58.9 Å²
XLogP3-AA	2.7
H-bond Donor Count	2
H-bond Acceptor Count	4
Rotatable Bond Count	5
GI absorption	High
BBB permeant	Yes

MW, molecular weight; TPSA, Topological polar surface area; XLogP3-AA, computed oc-tanol/water partition coefficient; BBB permeant, blood brain barrier permeant.

gree value of 9 were obtained, in which ESR1, ERBB2, HSP90AA1, MAPK8, CDK4, XIAP, RPS6KB1, PTGS2, CDK1, IGF1R, ABL1, PARP1, and CHEK1 were selected (Fig. 2C) (Table 2). Then, we further analyzed the high score proteins using the *cytoNCA* plug-in and obtained 13 nodes with 58 edges and an average degree value of 8.9. Three targets, HSP90AA1, XIAP, and ESR1, were identified as occupying a central position in the PPI network and were expected to serve as key core targets (Fig. 2D).

3.3 GO and pathway analysis

GO enrichment analysis was performed on 32 intersecting targets using the *R* language package. A total of 707 biological process (BP) entries were obtained, involving peptidyl-serine modification, regulation of cell cycle G2/M phase transition, peptidyl-serine phosphorylation, regulation of protein kinase B signaling, signal transduction in re-

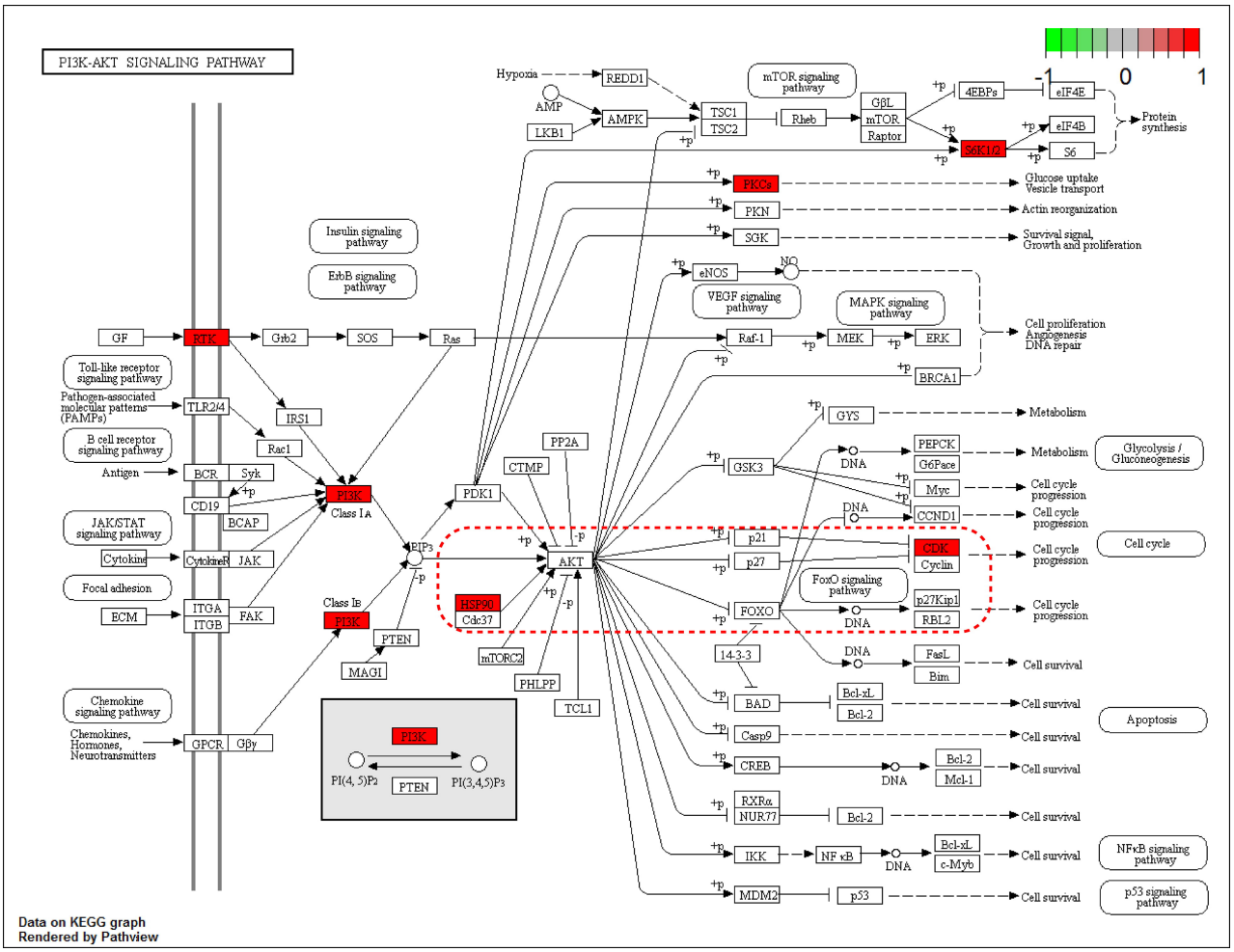

Fig. 4. The PI3K-Akt signaling pathway. The nodes marked in red are target genes. The red dashed box highlights our predicted key drug targets in the PI3K-Akt pathway. HSP90 may be one of the targets for the action of gigantol. HSP90/Akt/CDK1 is the likely downstream pathway of interest. Using *R* packages ("*pathview*").

sponse to DNA damage and other processes. Thirty seven cellular component (CC) entries were obtained, involving the pigment granule membrane, nuclear chromosome, telomeric region, cyclin-dependent protein kinase holoenzyme complex, and other components. Forty two molecular function (MF) entries involved nuclear receptor binding, transmembrane receptor protein tyrosine kinase activity, and cyclin-dependent protein kinase activity. The top 10 entries of the 3 cluster analyses were plotted according to the number of genes sorted (see Fig. 3A). KEGG enrichment analysis was performed on 32 intersecting targets with the *R* package. A total of 106 entries were obtained, and the results suggested that genes were predominantly enriched in the PI3K-Akt signaling pathway, endocrine resistance, ErbB signaling pathway, IL-17 signaling pathway, HIF-1 signaling pathway, and hepatocellular carcinoma, as shown in Fig. 3B (**Supplementary Table 2**). The results clearly revealed that the PI3K-Akt signaling pathway was more abundant among HCC-related pathways and had a critical role in the treatment of HCC (Fig. 4).

3.4 Docking results analysis

Whether a small molecule can bind to a large protein is mainly evaluated by the binding energy, which if it is less than 0, the ligand and the receptor can bind spontaneously. Smaller values indicate stronger binding capacity where the active ingredient binds to the receptor more easily. In this experiment, the average docking score of gigantol was used as the threshold value. The binding energy of the target protein to small molecules with a threshold value less than –5 kcal/mol was calculated. Three proteins were successfully docked with gigantol. The molecular docking results revealed that the binding energies of gigantol to the proteins ESR1, HSP90AA1, and XIAP were –6.5, –6.3, and –6.2 kcal/mol, respectively, indicating that the three molecules were highly active (Table 3). Affinity values <–7 suggest a relatively high binding activity [37]. Gigantol binds to ESR1 protein residues GLY521, HIS524, and LEU346 (Fig. 5A–B); to HSP90AA1 protein residues PHE138 and ASP93 by hydrogen bonding and van der Waals forces (Fig. 5C–D); and to XIAP protein residues

Table 2. Topological parameters of the 32 targets.

Name	Betweenness	Closeness	Degree	Eigenvector	LAC	Network
ESR1	119.458775	0.756097561	21	0.334978998	8.571428571	17.59735988
ERBB2	193.2986109	0.738095238	20	0.266285211	5.7	13.74281303
HSP90AA1	91.99843591	0.720930233	19	0.311388731	8.210526316	15.2760101
MAPK8	86.93683	0.688888889	17	0.249040633	6.588235294	13.0373002
CDK4	47.88048556	0.645833333	15	0.253567874	7.466666667	11.83308358
XIAP	18.81066257	0.645833333	14	0.271532387	8.571428571	10.71085859
RPS6KB1	35.45680286	0.62	13	0.220462099	5.846153846	7.91991342
PTGS2	35.8962606	0.62	13	0.197408468	6.307692308	10.29350649
CDK1	15.60249175	0.58490566	12	0.217495233	7.833333333	9.890909091
IGF1R	26.57395043	0.607843137	12	0.197221518	6	8.968181818
ABL1	24.98813008	0.607843137	11	0.204987556	6	7.655555556
PARP1	15.52287496	0.607843137	11	0.214561418	6.909090909	8.319444444
CHEK1	8.966233354	0.574074074	11	0.204811394	7.454545455	8.946031746
CDK2	1.773809524	0.553571429	10	0.195786715	7.8	8.968253968
AURKA	0.571428571	0.543859649	9	0.179965124	7.555555556	8.607142857
PLK1	7.201731602	0.534482759	8	0.147147462	5.5	6.392857143
ESR2	2.252380952	0.563636364	8	0.158232242	5.75	6.8
MMP7	5.584594817	0.553571429	7	0.109712064	5.142857143	6.333333333
MMP1	5.584594817	0.553571429	7	0.109712064	5.142857143	6.333333333
MMP3	10.06937866	0.508196721	7	0.093782939	4	5
PIK3CG	4.400582338	0.516666667	6	0.10157793	3	3.75
CYP19A1	1.203361345	0.534482759	6	0.117587544	4	4.8
RET	21.12384817	0.553571429	6	0.087166645	1.333333333	1.65
EPHB2	5.642857143	0.442857143	5	0.060849536	1.2	1.583333333
PIK3CD	2.692929293	0.492063492	5	0.072902597	2.4	3
MMP13	0	0.449275362	5	0.063357756	4	5
EPHA2	4.434199134	0.516666667	4	0.070508458	2	2.666666667
NOS2	0.333333333	0.492063492	4	0.081238903	2.5	3.333333333
PRKCA	3.74042624	0.5	4	0.059561979	0.5	0.666666667
CSK	0	0.46969697	3	0.059485048	2	3
TYR	0	0.476923077	2	0.043449122	1	2
CXCR1	0	0.430555556	1	0.022233263	0	0

Table 3. Parameters of the grid box in molecular docking.

Targets	PDB ID	Grid center			Npts			Spacing	Binding energie
ESR1	2JFA	–35.047	17.223	–4.757	40	40	40	1.0	–6.5
HSP90AA1	3T0H	–0.802	–14.335	–20.396	40	40	40	1.0	–6.3
XIAP	4MTZ	9.296	–0.371	17.785	40	40	40	1.0	–6.2

GLN1074, TYR75, GLN3074, and ARG1072 (Fig. 5E–F). From the valence bonding point of view, these three proteins bind to gigantol via multiple valence bonds, indicating a high binding stability.

3.5 Gigantol inhibited the proliferation of HCC cells

The inhibition rates of gigantol on Hep3B, SMMC-7721, and HCC-LM3 cells are shown in Fig. 6A. For SMMC-7721 cells, the IC_{50} was 84.18 μM at 24 h, 66.90 μM at 48 h, and 57.95 μM at 72 h. For HCC-LM3 cells, the IC_{50} was 70.2 μM at 24 h, 46 μM at 48 h, and 60.21 μM at 72 h. For Hep3B cells, the IC_{50} was 70.2 μM at 24 h. Surprisingly, the IC_{50} decreased to 20.57 μM at 48 h and to 16.01 μM at 72 h. Thus, we selected Hep3B and SMMC-7721 cells for the next assays. EdU can be incorporated into newly synthesized DNA as a substitute for thymine during DNA synthesis. The newly synthesized DNA was labeled with the corresponding fluorescent probe, and proliferating cells were detected using fluorescent detection equipment. EdU staining assays further examined the proliferation inhi-

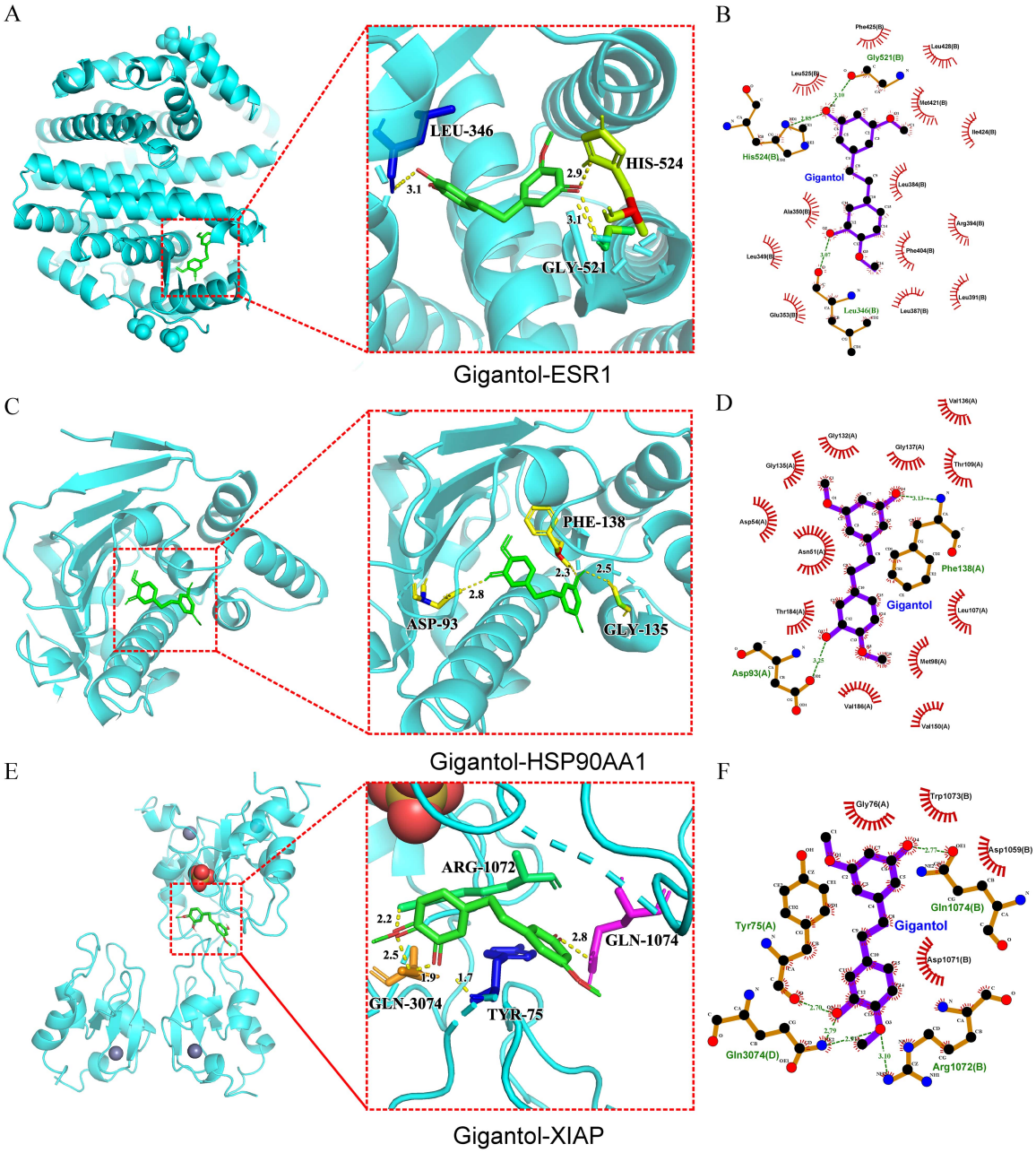

Fig. 5. Molecular docking. (A) 3D structural diagrams of the interactions between ESR1, HSP90AA1 (C), XIAP (E) with gigantol, respectively. (B) Plot of the distribution of the interaction forces between ESR1, HSP90AA1 (D), XIAP (F) and gigantol, individually.

bition ability of gigantol on hepatocellular carcinoma cells and demonstrated that EdU-positive cells were significantly reduced after treatment with different concentrations of gigantol compared to the control group (Fig. 6B–C).

3.6 Gigantol suppressed migration and invasion of cells

As shown in Fig. 7A–B, wound healing assays demonstrated that the scratches of gigantol treated Hep3B and SMMC-7721 cells were significantly larger than those of the control cells after 24 h. Additionally, the Matrigel invasion assay demonstrated that gigantol inhibited the invasion rate of Hep3B and SMMC-7721 cells compared to the control group (Fig. 7C–D). The aforementioned results demonstrated that gigantol could effectively inhibit the migration and invasion of HCC cells.

3.7 Effect of gigantol on the protein expression of PCNA, MCM2, E-cadherin, N-cadherin and Vimentin

To further determine the efficacy of gigantol, we assayed proliferation, migration and invasion related biomarkers. Following gigantol intervention, PCNA and MCM2 secretion was significantly diminished in the experimental group compared to the control group. Stimulation with different concentrations of gigantol (0, 25, 50, 100

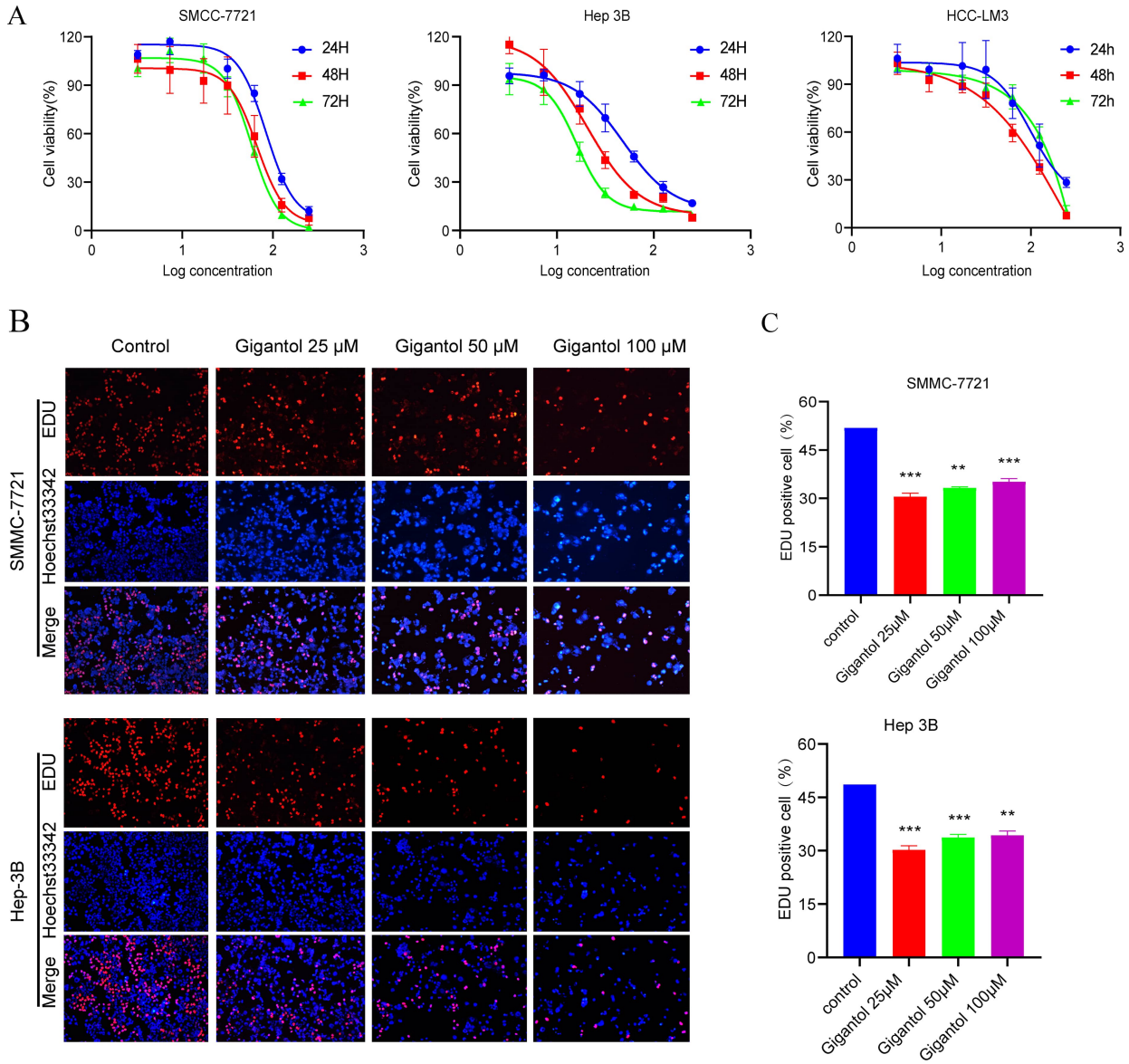

Fig. 6. Gigantol inhibits the proliferation of HCC cells. (A) The viability of SMMC-7721, Hep3B and HCC-LM3 cells treated with different concentrations of gigantol for 24 h, 48 h and 72 h was examined by CCK-8 assay. (B) The multiplicative capacity of SMMC-7721 and Hep 3B cells was decreased after different concentrations of gigantol intervention for 24 h. (C) Bar graphs show the percentage of EdU-positive cells in SMMC-7721 ($p < 0.001$) and Hep3B cells ($p < 0.01$).

μM) showed a pronounced decrease in a dose-dependent manner. For migration and invasion related proteins, the experimental group significantly inhibited N-cadherin and vimentin protein expression after treatment with different doses of gigantol, while the level of E-cadherin was significantly increased (Fig. 8).

3.8 Effect of gigantol on drug targets and HSP90/Akt/CDK1 signaling pathway

To verify the regulatory effect of gigantol on target proteins, we examined the changes of protein levels after gigantol intervention. As can be seen from Fig. 9, the expression levels of ESR1, HSP90AA1, and XIAP were gradually depressed with the increase of drug concentration. Combined with the results obtained in Fig. 4, we found that the drug target HSP90 protein is the upstream regulator of Akt. Therefore, we tentatively examined the changes of downstream p-Akt, Akt and CDK1 protein levels. As expected, we found that the levels of p-Akt and CDK1 were subsequently altered after drug intervention. This is consistent with the altered levels of the 3 targets.

4. Discussion

In this study, a “drug-target-disease” network was constructed using network pharmacology to explore the mechanism of gigantol in the treatment of HCC. Gigan-

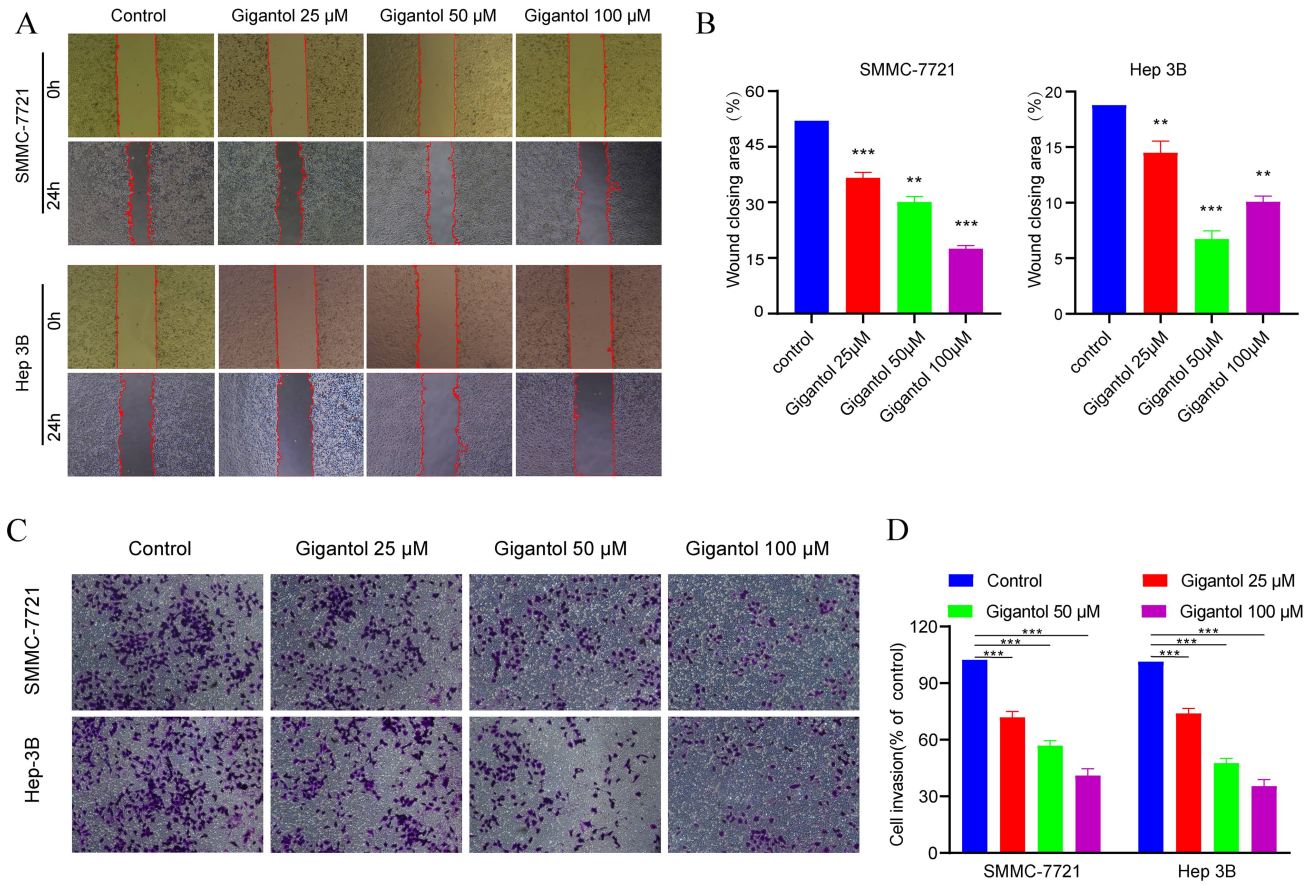

Fig. 7. Gigantol suppressed migration and invasion of cells. (A) The representative micrographs of "wound healing assay" of SMMC-7721 cells and Hep3B cells after 24 h are shown. (B) Bar graphs show the percentage of the area for the scratched region in SMMC-7721 ($p < 0.001$) and Hep3B cells ($p < 0.01$). (C,D) After intervention with gigantol, the invasive ability and number of invaded SMMC-7721 and Hep3B cells were evaluated by Transwell invasion assay.

tol can exert its efficacy in the treatment of HCC through multiple targets and pathways (Fig. 10). The results of network pharmacology analysis demonstrated that there were 32 targets related to gigantol, corresponding to 30 significant signaling pathways, including tumorigenesis, the cell cycle and immune regulation.

The bioavailability of gigantol is high, and it is known from the SwissADME results that gigantol is easily absorbed through the gastrointestinal tract. In drug likeness, Lipinski, Ghose, Veber, Egan, and Muegge scores were high. Some studies reported that gigantol could inhibit the metastasis of human bladder cancer cells through the Wnt/EMT signaling pathway [37]. One study found that gigantol could inhibit the proliferation of lung cancer by enhancing the GSK3-β-mediated ubiquitin proteasome and reducing MYC proto-oncogene (MYC) stabilization [38]. By mass spectrometry, one study identified c-Met as a protein target for gigantol to inhibit lung cancer metastasis [39]. In hepatocellular carcinoma, some studies reported that gigantol could inhibit the proliferation of hepatocellular carcinoma HepG2 cells through the PI3K/Akt/NF-κB signaling pathway [40]. In conclusion, gigantol is an excellent drug candidate because it is readily soluble, absorbable, safe, and nontoxic. Our results show that gigantol has significant effects in suppressing tumor proliferation and metastasis, not only in promoting apoptosis. Such a conclusion was verified simultaneously at the protein level and functional phenotype. We derived the same results from parallel validation in Hep3B and SMMC-7721 cells. In future research, this investigation should be extended to non-cancer hepatocytes or other cells from different tissues. However, the two cell lines are other than that studied but agree with the findings of Chen *et al.* [40]. In general, the low IC_{50} value of gigantol and its good water solubility and gastrointestinal absorption deserve to be studied in depth.

The results of KEGG pathway analysis showed that signaling pathways, such as the PI3K/Akt signaling pathway, cancer pathway, IL-17 signaling pathway, and HIF-1 signaling pathway, were significantly different. Among these pathways, the PI3K/Akt signaling pathway and HIF-1 signaling pathway are closely related to the occurrence of HCC. The PI3K/Akt signaling pathway is an important pathway for transmitting extracellular signals to the nucleus. Akt is an important link between intracellular growth

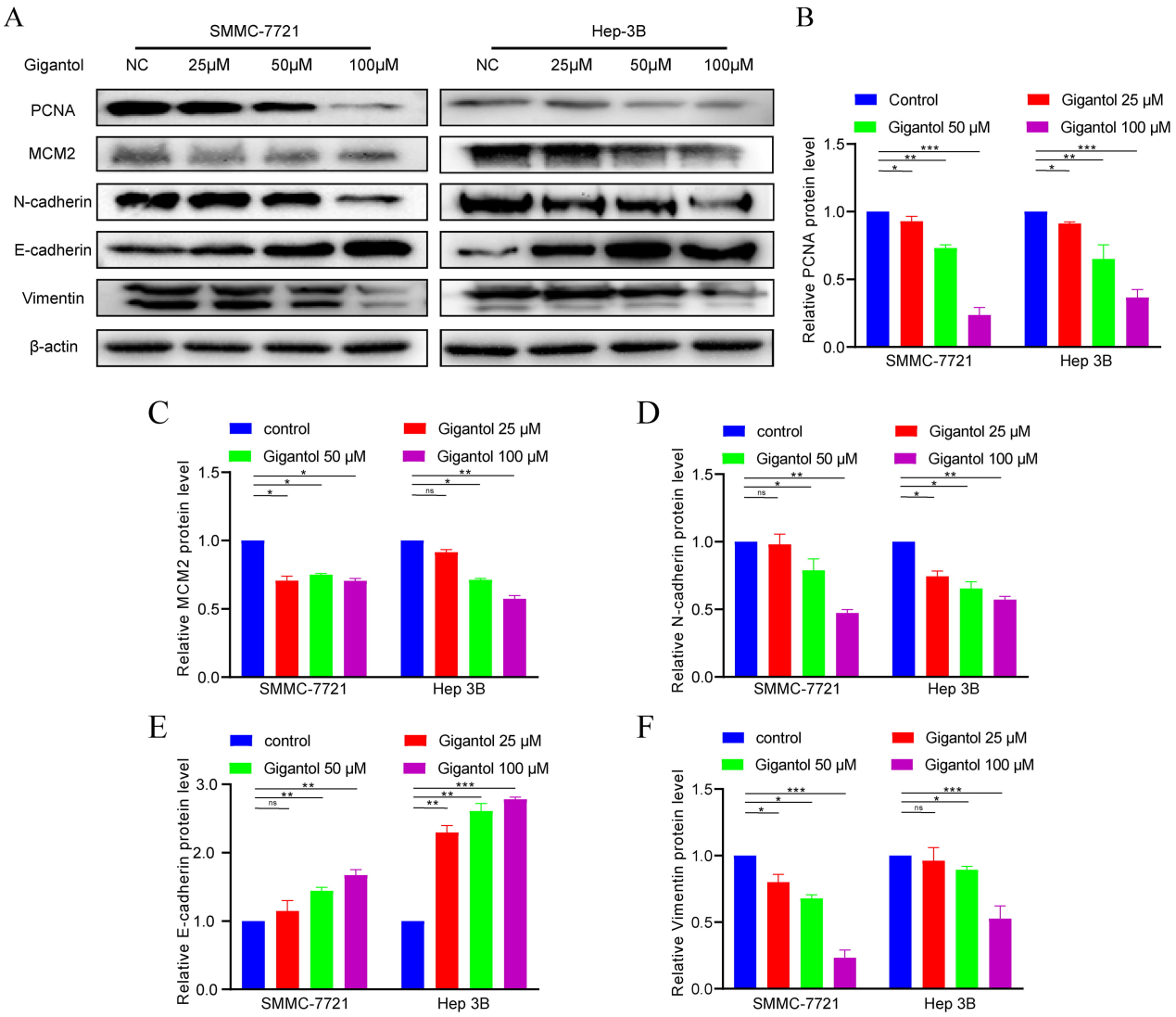

Fig. 8. Effects of gigantol on biomarkers of Phenotypes. (A,B,C) (D,E,F) Detection of proliferation and EMT biomarkers using western blot analysis. Data of quantifiable western blot assays.

regulation and glucose metabolism and plays an important regulatory role in various biological activities, such as cell proliferation, apoptosis, survival and metabolism [41]. Akt is an important downstream mediator of the PI3K promoter. After phosphorylation activation, PI3K regulates the expression of various genes, such as those related to apoptosis, the cell cycle and metabolism, by regulating downstream targets FOXO-1 and GSK-3 [42]. HIF-1α, an important hypoxia-inducible factor, plays an important role in this process. HIF-1α, stimulated by oncogenes, hypoxia and growth factors, can accumulate in the cytoplasm and translocate to the nucleus to bind to HIF-1β, which activates to become HIF-1 with full transcriptional function [43]. Studies have shown that upregulation of HIF-1 activity can lead to increased cell survival in hypoxic and local ischemic conditions and massive angiogenesis of hypoxic tissues; conversely, the use of its inhibitors can prevent angiogenesis and thus reduce the viability of hypoxic or inflammatory tissues [44]. Previous studies have reported that gigantol can promote apoptosis in hepatocellular carcinoma cells through PI3K/Akt/NF-κB signaling pathway [40]. In addition, some studies reported that the phosphorylation level of Akt decreased after specific inhibition of HSP90 protein and its activity was reduced [45]. Our study found that Akt can play a role in regulating tumor proliferation, metastasis, and regulating cell cycle as a downstream of HSP90. After gigantol interfered with the target HSP90, the downstream p-Akt changed consistently. As a result, Akt can play a role in regulating cell cycle. Gigantol interfered with the target HSP90 and showed consistent changes in downstream p-Akt. We speculate that gigantol may regulate the phosphorylation process of Akt through HSP90. CDK1, a downstream protein of Akt, also undergoes the same changes after drug intervention. Therefore, we speculate that gigantol may regulate the growth of hepatocellular carcinoma cells through HSP90/Akt/CDK1.

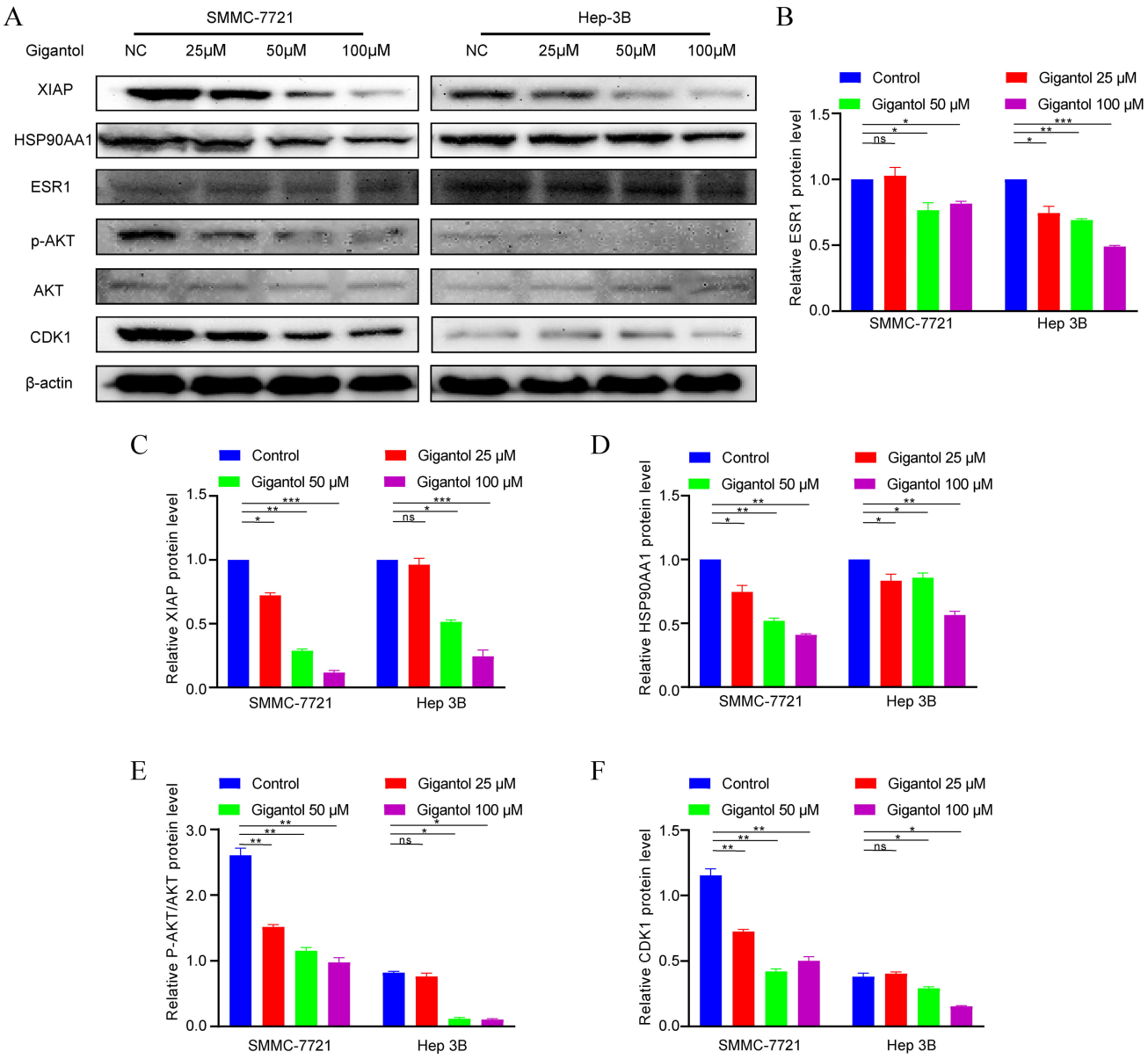

Fig. 9. Effects of gigantol on drug targets and HSP90/Akt/CDK1 signaling pathway. (A,B,C,D,E,F) Detection of ESR1, HSP90AA1, XIAP, p-Akt, Akt and CDK1 using western blot analysis. Data of quantifiable western blot assays.

The PPI network showed that the 13 node degree values of ABL1, RPS6KB1, CDK4, ERBB2, HSP90AA1, XIAP, CDK1, ESR1, MAPK8, PARP1, CHEK1, IGF1R and PTGS2 were significantly higher than those of the other targets. Among them, the target proteins ESR1, XIAP and HSP90AA1 appear to be the most relevant and play a crucial role. Abnormal expression of the estrogen receptor 1 gene can promote a variety of liver diseases, such as chronic alcoholic liver disease [46], HBV-related cirrhosis [47], benign liver adenoma [48], and malignant liver cancer, and even affect the therapeutic effect of entecavir [49]. Compared with normal individuals, patients with liver cancer are more likely to have mutations and abnormal expression of the ESR1 gene. ESR1 mutations may be an important marker in the progression of liver disease, and HBV carriers with ESR1 mutations have a higher probability of developing malignant changes [50].

X-linked inhibitor of apoptosis protein (XIAP) is a member of the inhibitor of apoptosis family of proteins (IAPs). XIAP is the most prevalent and potent apoptosis inhibitor protein in the IAP family. XIAP contains a ring-finger structure with ubiquitin ligase (E3) activity. The E3 ligase of XIAP can upregulate cell cycle protein D1 transcription through transactivation of c-Jun/AP-1, which in turn affects the signaling cascade responses of apoptosis, proliferation and migration [51]. In contrast, when XIAP expression was down-regulated, cell cycle protein D1 expression was reduced and cell proliferation was attenuated [52]. In addition, XIAP promotes the proliferation of hepatocellular carcinoma cells by regulating the expres-

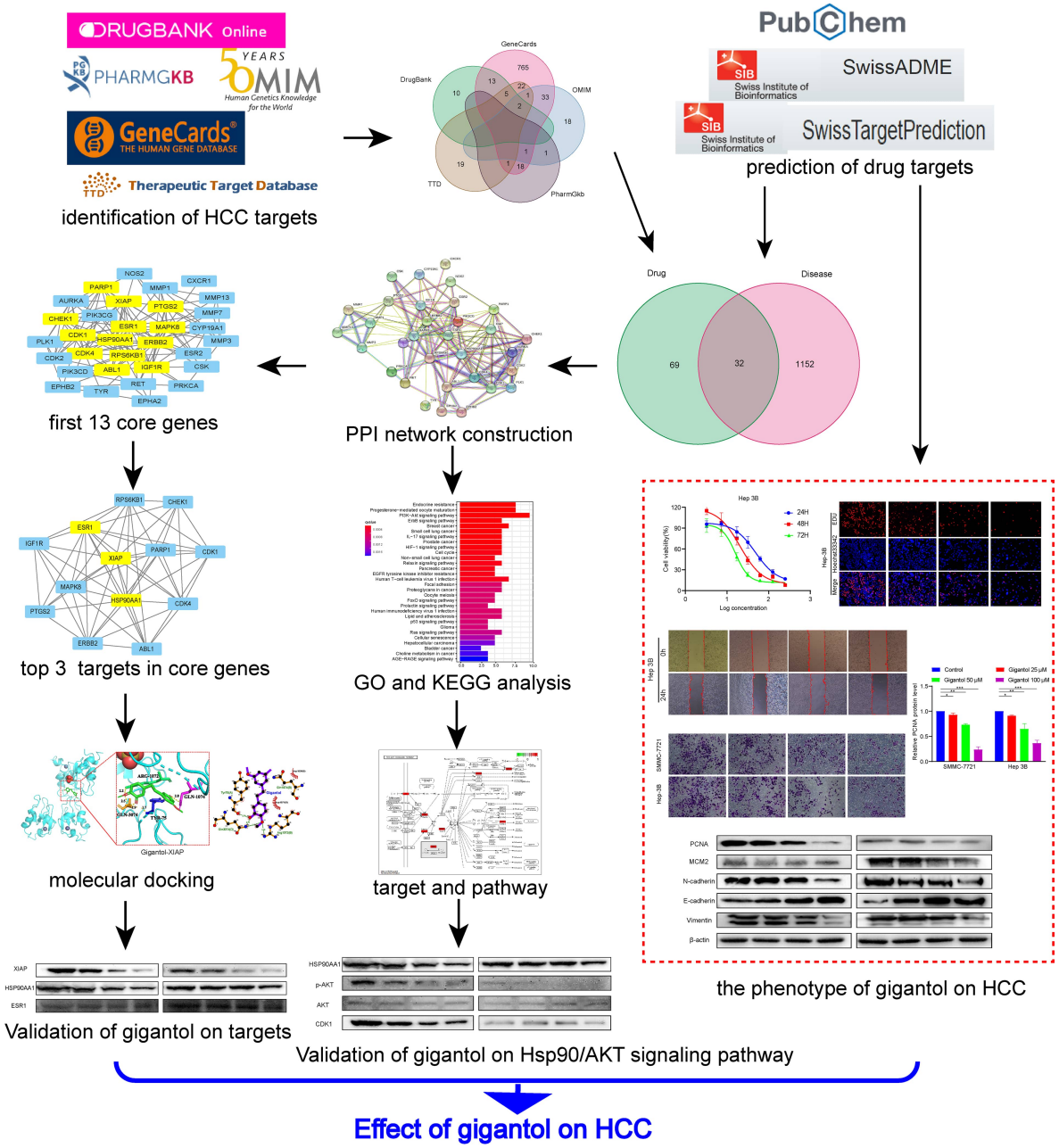

Fig. 10. Workflow of network pharmacology analysis of gigantol against HCC. Through database mining, a series of online tools, two categories of targets were identified, including (1) Targets of gigantrol, and (2) genes associated with HCC. The intersection of these two sets of targets may be part of the potential therapeutic targets for hepatocellular carcinoma. Then, PPI, KEGG, and GO analyses were performed for all the obtained targets. In addition, molecular docking was performed to predict the possible targets of action. Finally, the phenotype and HSP90/Akt/CDK1 pathway effects of gigantol on the role of HCC were verified.

sion of the CDK4/CDK6/CyclinD1 complex. After treatment of hepatocellular carcinoma cells with embelin (an XIAP-specific inhibitor), tumor cell proliferation was significantly inhibited [53,54].

The heat shock protein (HSP) family consists of molecular chaperone proteins that play an important role in tumor development. Studies have shown that HSP90 can play a role in inhibiting apoptosis, regulating cell division and promoting angiogenesis [55]. Further studies have revealed that HSP90 is highly expressed in a variety of tumors, such as lung and liver cancers [56,57]. As an important member of this family, HSP90AA1 has been shown to have pro-proliferative and prognostic effects in tumors such as breast cancers [58]. HSP90 plays a key role in the conformational maturation of oncogenic signaling proteins, among them HER-2/ErbB2, Akt, Raf-1, Bcr-Abl, and mutant P53, as a molecular chaperone [59,60]. HSP90, has an essential role in the PI3K/Akt/mTOR complex of

the PI3K/Akt signaling pathway to promote endothelial cell survival as a key protein chaperone [61,62]. Our results revealed that PI3K/Akt pathway is one of the key pathways interrupted by gigantol in hepatocellular carcinoma. Further analyzing with the molecular docking results, we found that HSP90 is the protein playing a key role in the PI3K/Akt pathway. We further explored the role of HSP90/Akt and downstream protein CDK1 on this work and validated the results from *in vitro* experiments.

The molecular docking results indicated that gigantol could bind stably to the core target proteins ESR1, XIAP and HSP90AA1, indicating that gigantol may regulate cell proliferation and apoptosis by acting on these targets to modulate immune activity and thus treat HCC. The same conclusion can be tentatively drawn from our western blotting validation results. Among them, gigantol has the strongest ability to regulate XIAP protein. In addition, the results from in vitro experiments showed that gigantol inhibited the growth, invasion, and metastasis of hepatocellular carcinoma cells in a dose-dependent manner. Additionally, we detected the expression of related marker proteins using western blotting, all of which yielded similar results. We verified from molecular docking and protein level that gigantol can exert regulatory effects through three targets, ESR1, XIAP and HSP90AA1, but it is never enough. In the future, it is worthwhile to further resolve the structure by cryoelectron microscopy or X-ray diffraction crystals.

In conclusion, gigantol has multiple effects, such as tumor regulation and immune modulation, and is mainly used to treat HCC by regulating the expression of related proteins through the multiple above mentioned components, targets and pathways. However, Chinese medicine is a complex multicomponent system. The present study only confirmed the mechanism of gigantol in the treatment of liver cancer from a microscopic perspective. Nevertheless, the study lacks data for *in vivo* experimental validation. Follow-up studies will be conducted based on the present study to evaluate gigantol's clinical application.

5. Conclusions

Our findings suggest that gigantol can treat hepatocellular carcinoma through mechanisms predicted by network pharmacology, such as inhibition of Hep3B and SMMC-7721 cell proliferation, invasion, metastasis and expression of related proteins. These findings provide potential molecular and cellular evidence that gigantol may be a promising antitumor agent. In addition, we preliminarily confirmed three key drug targets of gigantol, which are ESR1, HSP90AA1 and XIAP. Further explored that gigantol may exert its effects through the HSP90/Akt/CDK1 signaling pathway.

Abbreviations

HCC, Hepatocellular carcinoma; RFA, Radiofrequency ablation; TACE, Transarterial chemoembolization; Akt, Protein kinase B; OCT4, Organic cation/carnitine transporter 4; Nanog, Nanog homeobox; BBB, Blood brain barrier; GO, Gene ontology; BP, Biological process; CC, Cellular component; MF, Molecular function; KEGG, Kyoto encyclopedia of genes and genomes; PI3K, Phosphatidylinositol-4,5-Bisphosphate 3-Kinase; ErbB, Epidermal growth factor receptor (EGFR); ESR1, Estrogen receptor 1; HSP90AA1, Heat shock protein 90 alpha family class a member 1; XIAP, X-linked inhibitor of apoptosis; PCNA, Proliferating cell nuclear antigen; MCM2, Minichromosome maintenance complex component 2; CDK1, Cyclin dependent kinase 1.

Author contributions

SL, HL—conceptualization, methodology, visualization, data curation, writing original draft; SL, DY, XX, XL, XC—software, data curation; JL, XX, HL—validation, writing, review, editing; YY—supervision, project administration; All authors contributed to editorial changes in the manuscript. All authors read and approved the final manuscript.

Ethics approval and consent to participate

Not applicable.

Acknowledgment

We sincerely appreciate the technical support from Nanjing University of Chinese Medicine.

Funding

This study was funded by the Fujian Province Key Specialties in Traditional Chinese Medicine Construction Project (No. Fujian Health Chinese Medicine Letter (2019) No.262), the Jiangsu Province condition construction and livelihood science technologic special funds (BL2014005), the Startup Fund for scientific research, Fujian Medical University (Grant number: 2020QH1080), the 2021 Jiangsu Postgraduate Research and Practice Innovation Program of Postgraduate Training Innovation Project (SJCX21_0761), and Medical Science and Technology Development Foundation, Nanjing Department of Health (YKK19112).

Conflict of interest

The authors declare no conflict of interest.

Supplementary material

Supplementary material associated with this article can be found, in the online version, at https://www.imrpress.com/journal/FBL/27/1/10.31083/j.fbl2701025.

References

[1] Bray F, Ferlay J, Soerjomataram I, Siegel RL, Torre LA, Jemal A. Global cancer statistics 2018: GLOBOCAN estimates of in-

cidence and mortality worldwide for 36 cancers in 185 countries. CA: A Cancer Journal for Clinicians. 2018; 68: 394–424.
[2] Sapisochin G, Barry A, Doherty M, Fischer S, Goldaracena N, Rosales R, *et al*. Stereotactic body radiotherapy vs. TACE or RFA as a bridge to transplant in patients with hepatocellular carcinoma. an intention-to-treat analysis. Journal of Hepatology. 2017; 67: 92–99.
[3] Wang W, Wang Z, Wu J, Zhang T, Rong W, Wang L, *et al*. Survival benefit with IMRT following narrow-margin hepatectomy in patients with hepatocellular carcinoma close to major vessels. Liver International. 2015; 35: 2603–2610.
[4] Chen M, Li J, Zheng Y, Guo R, Liang H, Zhang Y, *et al*. A Prospective Randomized Trial Comparing Percutaneous Local Ablative Therapy and Partial Hepatectomy for Small Hepatocellular Carcinoma. Annals of Surgery. 2006; 243: 321–328.
[5] Feng K, Yan J, Li X, Xia F, Ma K, Wang S, *et al*. A randomized controlled trial of radiofrequency ablation and surgical resection in the treatment of small hepatocellular carcinoma. Journal of Hepatology. 2012; 57: 794–802.
[6] Kim Y, Lim HK, Rhim H, Lee MW, Choi D, Lee WJ, *et al*. Ten-year outcomes of percutaneous radiofrequency ablation as first-line therapy of early hepatocellular carcinoma: Analysis of prognostic factors. Journal of Hepatology. 2013; 58: 89–97.
[7] Zhang L, Ge N, Chen Y, Xie X, Yin X, Gan Y, *et al*. Long-term outcomes and prognostic analysis of radiofrequency ablation for small hepatocellular carcinoma: 10-year follow-up in Chinese patients. Medical Oncology. 2015; 32: 77.
[8] Zhou C, Peng Y, Zhou K, Zhang L, Zhang X, Yu L, *et al*. Surgical resection plus radiofrequency ablation for the treatment of multifocal hepatocellular carcinoma. HepatoBiliary Surgery and Nutrition. 2019; 8: 19–28.
[9] Ikeda M, Kudo M, Aikata H, Nagamatsu H, Ishii H, Yokosuka O, *et al*. Transarterial chemoembolization with miriplatin vs. epirubicin for unresectable hepatocellular carcinoma: a phase III randomized trial. Journal of Gastroenterology. 2018; 53: 281–290.
[10] Lencioni R, de Baere T, Soulen MC, Rilling WS, Geschwind JH. Lipiodol transarterial chemoembolization for hepatocellular carcinoma: a systematic review of efficacy and safety data. Hepatology. 2016; 64: 106–116.
[11] Wang Z, Ren Z, Chen Y, Hu J, Yang G, Yu L, *et al*. Adjuvant Transarterial Chemoembolization for HBV-Related Hepatocellular Carcinoma after Resection: a Randomized Controlled Study. Clinical Cancer Research. 2018; 24: 2074–2081.
[12] Cheng A, Kang Y, Chen Z, Tsao C, Qin S, Kim JS, *et al*. Efficacy and safety of sorafenib in patients in the Asia-Pacific region with advanced hepatocellular carcinoma: a phase III randomised, double-blind, placebo-controlled trial. The Lancet Oncology. 2009; 10: 25–34.
[13] Harnois DM. Sorafenib in Advanced Hepatocellular Carcinoma. Yearbook of Medicine. 2009; 2009: 459–461.
[14] Kudo M, Finn RS, Qin S, Han K, Ikeda K, Piscaglia F, *et al*. Lenvatinib versus sorafenib in first-line treatment of patients with unresectable hepatocellular carcinoma: a randomised phase 3 non-inferiority trial. The Lancet. 2018; 391: 1163–1173.
[15] Qin S, Bai Y, Lim HY, Thongprasert S, Chao Y, Fan J, *et al*. Randomized, Multicenter, Open-Label Study of Oxaliplatin Plus FluorouracilLeucovorin Versus Doxorubicin as Palliative Chemotherapy in Patients with Advanced Hepatocellular Carcinoma from Asia. Journal of Clinical Oncology. 2013; 31: 3501–3508.
[16] Qin S, Cheng Y, Liang J, Shen L, Bai Y, Li J, *et al*. Efficacy and Safety of the FOLFOX4 Regimen Versus Doxorubicin in Chinese Patients with Advanced Hepatocellular Carcinoma: a Subgroup Analysis of the each Study. The Oncologist. 2014; 19: 1169–1178.
[17] Zhu Q, Sheng Y, Li W, Wang J, Ma Y, Du B, *et al*. Erianin, a novel dibenzyl compound in Dendrobium extract, inhibits bladder cancer cell growth via the mitochondrial apoptosis and JNK pathways. Toxicology and Applied Pharmacology. 2019; 371: 41–54.
[18] Wu J, Lu C, Li X, Fang H, Wan W, Yang Q, *et al*. Synthesis and Biological Evaluation of Novel Gigantol Derivatives as Potential Agents in Prevention of Diabetic Cataract. PLoS ONE. 2015; 10: e0141092.
[19] Bhummaphan N, Chanvorachote P. Gigantol Suppresses Cancer Stem Cell-Like Phenotypes in Lung Cancer Cells. Evidence-Based Complementary and Alternative Medicine. 2015; 2015: 836564.
[20] Unahabhokha T, Chanvorachote P, Pongrakhananon V. The attenuation of epithelial to mesenchymal transition and induction of anoikis by gigantol in human lung cancer H460 cells. Tumor Biology. 2016; 37: 8633–8641.
[21] Xiang Y, Guo Z, Zhu P, Chen J, Huang Y. Traditional Chinese medicine as a cancer treatment: Modern perspectives of ancient but advanced science. Cancer Medicine. 2019; 8: 1958–1975.
[22] Zuo H, Zhang Q, Su S, Chen Q, Yang F, Hu Y. A network pharmacology-based approach to analyse potential targets of traditional herbal formulas: an example of Yu Ping Feng decoction. Scientific Reports. 2018; 8: 11418.
[23] Zeng L, Yang K. Exploring the pharmacological mechanism of Yanghe Decoction on her2-positive breast cancer by a network pharmacology approach. Journal of Ethnopharmacology. 2017; 199: 68–85.
[24] Jing C, Sun Z, Xie X, Zhang X, Wu S, Guo K, *et al*. Network pharmacology-based identification of the key mechanism of Qinghuo Rougan Formula acting on uveitis. Biomedicine & Pharmacotherapy. 2019; 120: 109381.
[25] Kim S, Chen J, Cheng T, Gindulyte A, He J, He S, *et al*. PubChem in 2021: new data content and improved web interfaces. Nucleic Acids Research. 2021; 49: D1388-D1395.
[26] Daina A, Michielin O, Zoete V. SwissADME: a free web tool to evaluate pharmacokinetics, drug-likeness and medicinal chemistry friendliness of small molecules. Scientific Reports. 2017; 7: 42717.
[27] Stelzer G, Rosen N, Plaschkes I, Zimmerman S, Twik M, Fishilevich S, *et al*. The GeneCards Suite: from Gene Data Mining to Disease Genome Sequence Analyses. Current Protocols in Bioinformatics. 2016; 54: 1.30.1–1.30.33.
[28] Amberger JS, Bocchini CA, Schiettecatte F, Scott AF, Hamosh A. OMIM.org: Online Mendelian Inheritance in Man (OMIM(R)), an online catalog of human genes and genetic disorders. Nucleic Acids Research. 2015; 43: D789–798.
[29] Whirl-Carrillo M, McDonagh EM, Hebert JM, Gong L, Sangkuhl K, Thorn CF, *et al*. Pharmacogenomics Knowledge for Personalized Medicine. Clinical Pharmacology & Therapeutics. 2012; 92: 414–417.
[30] Wang Y, Zhang S, Li F, Zhou Y, Zhang Y, Wang Z, *et al*. Therapeutic target database 2020: enriched resource for facilitating research and early development of targeted therapeutics. Nucleic Acids Research. 2020; 48: D1031–D1041.
[31] Wishart DS, Feunang YD, Guo AC, Lo EJ, Marcu A, Grant JR, *et al*. DrugBank 5.0: a major update to the DrugBank database for 2018. Nucleic Acids Research. 2018; 46: D1074–D1082.
[32] Szklarczyk D, Gable AL, Lyon D, Junge A, Wyder S, Huerta-Cepas J, *et al*. STRING v11: protein–protein association networks with increased coverage, supporting functional discovery in genome-wide experimental datasets. Nucleic Acids Research. 2019; 47: D607–D613.
[33] Shannon P, Markiel A, Ozier O, Baliga NS, Wang JT, Ramage D, *et al*. Cytoscape: a Software Environment for Integrated Models of Biomolecular Interaction Networks. Genome Research. 2003; 13: 2498–2504.

[34] Burley SK, Bhikadiya C, Bi C, Bittrich S, Chen L, Crichlow GV, *et al*. RCSB Protein Data Bank: powerful new tools for exploring 3D structures of biological macromolecules for basic and applied research and education in fundamental biology, biomedicine, biotechnology, bioengineering and energy sciences. Nucleic Acids Research. 2021; 49: D437–D451.
[35] Morris GM, Huey R, Lindstrom W, Sanner MF, Belew RK, Goodsell DS, *et al*. AutoDock4 and AutoDockTools4: Automated docking with selective receptor flexibility. Journal of Computational Chemistry. 2009; 30: 2785–2791.
[36] Trott O, Olson AJ. AutoDock Vina: Improving the speed and accuracy of docking with a new scoring function, efficient optimization, and multithreading. Journal of Computational Chemistry. 2010; 31: 455–461.
[37] Zhao M, Sun Y, Gao Z, Cui H, Chen J, Wang M, *et al*. Gigantol Attenuates the Metastasis of Human Bladder Cancer Cells, Possibly Through Wnt/EMT Signaling. OncoTargets and Therapy. 2020; 13: 11337–11346.
[38] Losuwannarak N, Roytrakul S, Chanvorachote P. Gigantol Targets MYC for Ubiquitin-proteasomal Degradation and Suppresses Lung Cancer Cell Growth. Cancer Genomics - Proteomics. 2020; 17: 781–793.
[39] Aksorn N, Losuwannarak N, Tungsukruthai S, Roytrakul S, Chanvorachote P. Analysis of the Protein–Protein Interaction Network Identifying c-Met as a Target of Gigantol in the Suppression of Lung Cancer Metastasis. Cancer Genomics - Proteomics. 2021; 18: 261–272.
[40] Chen H, Huang Y, Huang J, Lin L, Wei G. Gigantol attenuates the proliferation of human liver cancer HepG2 cells through the PI3K/Akt/NF-kappaB signaling pathway. Oncology Reports. 2017; 37: 865–870.
[41] Mendoza MC, Er EE, Blenis J. The Ras-ERK and PI3K-mTOR pathways: cross-talk and compensation. Trends in Biochemical Sciences. 2011; 36: 320–328.
[42] Xu T, Pang Q, Wang Y, Yan X. Betulinic acid induces apoptosis by regulating PI3K/Akt signaling and mitochondrial pathways in human cervical cancer cells. International Journal of Molecular Medicine. 2017; 40: 1669–1678.
[43] Cheng J, Kang X, Zhang S, Yeh ET. SUMO-specific protease 1 is essential for stabilization of HIF1alpha during hypoxia. Cell. 2007; 131: 584–595.
[44] Silletti S, Paku S, Raz A. Tumor cell motility and metastasis. Pathology & Oncology Research. 1997; 3: 230–254.
[45] Basso AD, Solit DB, Chiosis G, Giri B, Tsichlis P, Rosen N. Akt Forms an Intracellular Complex with Heat Shock Protein 90 (Hsp90) and Cdc37 and is Destabilized by Inhibitors of Hsp90 Function. Journal of Biological Chemistry. 2002; 277: 39858–39866.
[46] Villa E, Baldini GM, Rossini GP, Pasquinelli C, Melegari M, Cariani E, *et al*. Ethanol-induced increase in cytosolic estrogen receptors in human male liver: a possible explanation for biochemical feminization in chronic liver disease due to alcohol. Hepatology. 1988; 8: 1610–1614.
[47] Yan Z, Tan W, Xu B, Dan Y, Zhao W, Deng C, *et al*. A cis-acting regulatory variation of the estrogen receptor alpha (ESR1) gene is associated with hepatitis B virus-related liver cirrhosis. Human Mutation. 2011; 32: 1128–1136.
[48] Porter LE, Elm MS, Van Thiel DH, Eagon PK. Hepatic estrogen receptor in human liver disease. Gastroenterology. 1987; 92: 735–745.
[49] Zhang TT, Ye J, Xia SL, Zhang YF, Su Q, Zhang ZH, *et al*. Polymorphism of estrogen receptor alpha (ESR1) is associated with virological response to entecavir (ETV) in nucleoside-naive adult patients with chronic hepatitis B. Infection. 2013; 41: 371–378.
[50] Villa E, Colantoni A, Grottola A, Ferretti I, Buttafoco P, Bertani H, *et al*. Variant estrogen receptors and their role in liver disease. Molecular and Cellular Endocrinology. 2002; 193: 65–69.
[51] Suzuki Y, Nakabayashi Y, Takahashi R. Ubiquitin-protein ligase activity of X-linked inhibitor of apoptosis protein promotes proteasomal degradation of caspase-3 and enhances its anti-apoptotic effect in Fas-induced cell death. Proceedings of the National Academy of Sciences. 2001; 98: 8662–8667.
[52] Cao Z, Zhang R, Li J, Huang H, Zhang D, Zhang J, *et al*. X-linked Inhibitor of Apoptosis Protein (XIAP) Regulation of Cyclin D1 Protein Expression and Cancer Cell Anchorage-independent Growth via its E3 Ligase-mediated Protein Phosphatase 2a/c-Jun Axis. Journal of Biological Chemistry. 2013; 288: 20238–20247.
[53] CHENG H, YANG H, YANG J, SUN A, CHEN H, YANG Xa, *et al*. Effects of microRNA-509-3p on proliferation and invasiveness of liver carcinoma HepG2 cells. Journal of Zhengzhou University (Medical Sciences). 2017; 52: 412–415.
[54] Huiyi H, Jianhui Y. The effects of XIAP siRNA and embelin on TRAIL-induced growth inhibition and apoptosis in hepatocarcinoma cells. Chinese Journal of Hepatobiliary Surgery. 2012; 18: 381–385.
[55] Chatterjee S, Burns TF. Targeting Heat Shock Proteins in Cancer: A Promising Therapeutic Approach. International Journal of Molecular Sciences. 2017; 18: 1978.
[56] CHEN Tian, TANG Z. Clinical significance of AFP-L3, Hsp90α test in the diagnosis of hepatocellular carcinoma with low and medium concentration of AFP. Chinese Journal of Cancer Prevention and Treatment. 2018; 25: 1511–1514.
[57] Minghui W, Lin F, Ping L, Naijun H, Yanning G, Ting X. Hsp90AB1 protein is overexpressed in non-small cell lung cancer tissues and associated with poor prognosis in lung adenocarcinoma patients. Chinese Journal of Lung Cancer. 2016; 19: 64–69.
[58] Liu H, Zhang Z, Huang Y, Wei W, Ning S, Li J, *et al*. Plasma HSP90AA1 Predicts the Risk of Breast Cancer Onset and Distant Metastasis. Frontiers in Cell and Developmental Biology. 2021; 9: 639596.
[59] Schulte TW, Blagosklonny MV, Ingui C, Neckers L. Disruption of the Raf-1-Hsp90 Molecular Complex Results in Destabilization of Raf-1 and Loss of Raf-1-Ras Association. Journal of Biological Chemistry. 1995; 270: 24585–24588.
[60] Xu W, Mimnaugh E, Rosser MFN, Nicchitta C, Marcu M, Yarden Y, *et al*. Sensitivity of Mature ErbB2 to Geldanamycin is Conferred by its Kinase Domain and is Mediated by the Chaperone Protein Hsp90. Journal of Biological Chemistry. 2001; 276: 3702–3708.
[61] Boucher M-J, Saryeddine L, Zibara K, Kassem N, Badran B, El-Zein N. EGF-Induced VEGF Exerts a PI3K-Dependent Positive Feedback on ERK and AKT through VEGFR2 in Hematological In Vitro Models. PLoS ONE. 2016; 11: e0165876.
[62] Xue Q, Nagy JA, Manseau EJ, Phung TL, Dvorak HF, Benjamin LE. Rapamycin Inhibition of the Akt/mTOR Pathway Blocks Select Stages of VEGF-A164–Driven Angiogenesis, in Part by Blocking S6Kinase. Arteriosclerosis, Thrombosis, and Vascular Biology. 2009; 29: 1172–1178.